



Published in final edited form as:

*NMR Biomed.* 2014 March ; 27(3): 356–362. doi:10.1002/nbm.3071.

## Hyperpolarized [1,4-<sup>13</sup>C]-Diethylsuccinate: A Potential DNP Substrate for In Vivo Metabolic Imaging

Kelvin L. Billingsley<sup>a,\*</sup>, Sonal Josan<sup>b,c</sup>, Jae Mo Park<sup>b</sup>, Sui Seng Tee<sup>b</sup>, Eleanor Spielman-Sun<sup>d</sup>, Ralph Hurd<sup>e</sup>, Dirk Mayer<sup>f</sup>, and Daniel Spielman<sup>b,g</sup>

<sup>a</sup>San Francisco State University, Department of Chemistry and Biochemistry, San Francisco, CA, 94132

<sup>b</sup>Stanford University, Department of Radiology, Stanford, CA 94305

<sup>c</sup>SRI International, Neuroscience Program, Menlo Park, CA 94025

<sup>d</sup>Oberlin College, Department of Chemistry, Oberlin, OH, 44074

<sup>e</sup>GE Healthcare, Applied Sciences Laboratory, Menlo Park, CA 94025

<sup>f</sup>University of Maryland-Baltimore, Department of Diagnostic Radiology and Nuclear Medicine, Baltimore, MD, 21201

<sup>g</sup>Stanford University, Department of Electrical Engineering, Stanford, CA 94305

### Abstract

The tricarboxylic acid cycle (TCA) performs an essential role in the regulation of energy and metabolism, and deficiencies in this pathway are commonly correlated with various diseases. However, the development of non-invasive techniques for the assessment of the cycle *in vivo* has remained challenging. In this work, the applicability of a novel imaging agent, [1,4-<sup>13</sup>C]-diethylsuccinate, for hyperpolarized <sup>13</sup>C metabolic imaging of the TCA cycle was explored. *In vivo* spectroscopic studies were conducted in conjunction with *in vitro* analyses to determine the metabolic fate of the imaging agent. Contrary to previous reports (Zacharias, N. M. et. al. *J. Am. Chem. Soc.* **2012**, *134*, 934-943), [<sup>13</sup>C]-labeled diethylsuccinate was primarily metabolized to succinate-derived products not originating from TCA cycle metabolism. These results illustrate potential issues of utilizing dialkyl ester analogs of TCA cycle intermediates as molecular probes for hyperpolarized <sup>13</sup>C metabolic imaging.

### Keywords

hyperpolarized carbon-13; dynamic nuclear polarization; magnetic resonance spectroscopy; tricarboxylic acid cycle

---

\*Correspondence to: Prof. Kelvin Billingsley, San Francisco State University, Department of Chemistry and Biochemistry, Thornton Hall 729, San Francisco, CA 94132, kllbillin@sfsu.edu, Phone: 415-405-0732, Fax: 415-338-2384.

## Introduction

Hyperpolarized  $^{13}\text{C}$  magnetic resonance spectroscopy (MRS) has shown considerable potential for disease diagnosis and treatment (1-10). This technique provides a complement to conventional metabolomic methods, adding real time dynamics at high spatial resolution. A key component of this emergent field is the development of novel molecular probes that can distinctly faster monitor these pathways. The tricarboxylic acid (TCA) cycle, in particular, has received significant attention as it plays a central role in cellular metabolism for the production of energy, and misregulation of the TCA cycle has increasingly been correlated with numerous diseases (11). For example, mutations in succinate dehydrogenase, fumarate hydratase, and isocitrate dehydrogenase are well-documented in tumorigenesis (12), and TCA cycle enzymes have been utilized as key biomarkers in cancer diagnosis (13-14). Furthermore, prolonged alterations in TCA cycle metabolism can result in deleterious modifications to mitochondrial energy production, which has been causally implicated in the progression of various neurological disorders (15-17).

Several strategies have been proposed for monitoring the efficiency of the TCA cycle via hyperpolarized  $^{13}\text{C}$  metabolic imaging. The most prominent method is the application of hyperpolarized  $[^{13}\text{C}]$ -pyruvate, which has typically been employed as an indirect marker of the pathway (Figure 1A).  $[1-^{13}\text{C}]$ -pyruvate is converted to acetyl-CoA, which can enter the cycle, and  $[^{13}\text{C}]$ -bicarbonate via pyruvate dehydrogenase (18-23). Although the detection of  $[^{13}\text{C}]$ -bicarbonate indicates flux into acetyl-CoA, this strategy does not provide any information pertaining to the TCA cycle and its intermediates. Alternatively, hyperpolarized  $[2-^{13}\text{C}]$ -pyruvate, which forms  $[1-^{13}\text{C}]$ -acetyl-CoA and subsequently integrates the label into TCA cycle intermediates, has been employed (24-25). However with the exception of citrate, only metabolites not on the TCA pathway (i.e.  $[5-^{13}\text{C}]$ -glutamate (24-26) and  $[1-^{13}\text{C}]$ -acetylcarnitine (27)) are regularly observed due in part to the relative rate of consumption of  $[2-^{13}\text{C}]$ -pyruvate by alternative pathways. Although  $[^{13}\text{C}]$ -pyruvate is metabolized by the TCA cycle, these probes have not been able to directly evaluate the catalytic activity of specific enzymes in the pathway.

Ongoing efforts are focused on the development of novel small molecule agents for monitoring TCA cycle metabolism that overcome the limitations associated with  $[^{13}\text{C}]$ -pyruvate. For example,  $[^{13}\text{C}]$ -labeled fumarate or succinate offers the advantage that they are primarily metabolized by the TCA cycle, whereas  $[^{13}\text{C}]$ -pyruvate can be diverted to several pathways (e.g. gluconeogenesis and fatty acid biosynthesis). Though both  $[^{13}\text{C}]$ -labeled fumarate (28-29) and succinate (30-31) derivatives have been successfully hyperpolarized, neither substrate is transported into the cytosol and mitochondria at a sufficient rate for evaluation within the 1-2 min  $T_1$ -limited time constraint of *in vivo* hyperpolarized  $^{13}\text{C}$  experiments. Hence, the utility of these agents, particularly fumarate (28-29), has been limited to assessing cell necrosis in which disruption of the cellular membranes allows TCA-cycle enzymes to leak into the extracellular space.

A recent method was reported for the direct monitoring of TCA cycle metabolism via hyperpolarized  $^{13}\text{C}$  MRS *in vivo*. This process relied upon the use of a new molecular probe,  $[1-^{13}\text{C}, 2,3-d_2]$ -diethylsuccinate, which was prepared via parahydrogen-induced polarization

(PHIP) from the corresponding [1-<sup>13</sup>C, 2,3-*d*<sub>2</sub>]-diethylfumarate (32). Diethylsuccinate (DES), thought to be easily transported across biological membranes, can then be converted *in vivo* to succinate (via monoethylsuccinate (MES) as an intermediate) by endogenous esterases (Figure 1B) (33-36). Upon entry into the mitochondria, succinate can then be metabolized by the TCA cycle and provide an analysis of the metabolic state in the intracellular environment. Importantly, this recent report utilizing PHIP hyperpolarized [1-<sup>13</sup>C, 2,3-*d*<sub>2</sub>]-diethylsuccinate was the first to suggest that various late-stage TCA cycle intermediates (e.g. fumarate and malate) could be monitored *in vivo*. Furthermore, aspartate, which plays a key role in the regulation of redox state in the mitochondria (37), was also detected. The PHIP method achieved a 2.1% + 0.6% of hyperpolarized [1-<sup>13</sup>C, 2,3-*d*<sub>2</sub>]-diethylsuccinate, and spectra were obtained from whole body of mice after either i.v. or i.p. injection of 20 mM substrate.

Dynamic Nuclear Polarization (DNP), which is widely employed for *in vivo* studies (38), also allows for substantial enhancement of nuclear polarization leading to improved detection limits for *in vivo* imaging and novel information concerning metabolic pathways. In this work, we explore the synthesis, development and application of [1,4-<sup>13</sup>C]-diethylsuccinate ([<sup>13</sup>C]-DES) as a DNP substrate for hyperpolarized <sup>13</sup>C metabolic imaging of the TCA cycle. These studies, which are the first to examine DES as a DNP agent, resulted in a reexamination of the *in vivo* metabolic fate of [<sup>13</sup>C]-labeled DES imaging agents.

## Experimental Details

### General

All reagents were purchased from Aldrich Chemical Co. unless otherwise noted and used without further purification.

### Synthesis of [1,4-<sup>13</sup>C]-Diethylsuccinate

[<sup>13</sup>C]-DES was prepared by the following procedure: In an oven-dried 100 mL round-bottom flask equipped with magnetic stir bar, 425 mg (3.54 mmol) of [1,4-<sup>13</sup>C]-succinic acid (99% 1,4-<sup>13</sup>C, CLM-1084, Cambridge Isotopes, Andover, MA) was added. After the addition of anhydrous ethanol (35 mL), 1.8 mL (1.54 g, 14.2 mmol) of trimethylsilyl chloride was added dropwise via syringe over the course of two minutes. The reaction was allowed to stir at room temperature. After 5 h, the reaction was quenched with 10 mL of saturated sodium bicarbonate solution. Additional bicarbonate was removed via filtration, and ethanol was removed under vacuum. The desired product was extracted from the aqueous solution with 4 x 8 mL of dichloromethane. Organic layers were combined, dried over anhydrous sodium sulfate, and filtered; the solvent was removed by evaporation and 480 mg (77% yield) of pure product was isolated as a colorless oil. <sup>1</sup>H NMR (CDCl<sub>3</sub>, 500 MHz) δ 4.15 (q, *J* = 7 Hz, 4H, -OCH<sub>2</sub>-), 2.60 (s, 4H, -C(O)CH<sub>2</sub>-), 1.12 (t, *J* = 7 Hz, 6H, -CH<sub>3</sub>) ppm; <sup>13</sup>C NMR (CDCl<sub>3</sub>, 125 MHz) δ 172.4 (-C(O)-), 60.8 (-OCH<sub>2</sub>-), 29.1 (-C(O)CH<sub>2</sub>-), 14.1 (-CH<sub>3</sub>) ppm.

### Synthesis of [1,4-<sup>13</sup>C]-Monoethylsuccinate

In order to reference [<sup>13</sup>C]-MES, a sample containing [<sup>13</sup>C]-succinate, [<sup>13</sup>C]-MES, and [<sup>13</sup>C]-DES was prepared by the following procedure: In an oven-dried 100 mL round-bottom flask equipped with magnetic stir bar, 100 mg (0.83 mmol) of [1,4-<sup>13</sup>C]-succinic acid was added. After the addition of anhydrous ethanol (5 mL), 0.106 mL (90.5 mg, 0.83 mmol) of trimethylsilyl chloride was added dropwise via syringe over the course of one minute. The reaction was allowed to stir at room temperature. After 30 min, the reaction was quenched with 2 mL of saturated sodium bicarbonate solution. Additional bicarbonate was removed via filtration, and ethanol was removed under vacuum. The desired product was extracted from the aqueous solution with 4 x 4 mL of dichloromethane. Organic layers were combined, dried over anhydrous sodium sulfate, and filtered; the solvent was removed by evaporation to yield a sample with 2:3:6 ratio of [<sup>13</sup>C]-succinate:[<sup>13</sup>C]-DES:[<sup>13</sup>C]-MES as determined by <sup>1</sup>H-NMR (D<sub>2</sub>O).

### Dynamic Nuclear Polarization of [1,4-<sup>13</sup>C]-Diethylsuccinate

The samples to be polarized consisted of 40 μL of a mixture of [<sup>13</sup>C]-DES (6 M, neat) and 20-mM α,γ-Bisdiphenylene-β-phenylallyl (BDPA) radical. The samples were polarized via dynamic nuclear polarization using a HyperSense system (Oxford Instruments Molecular Biotools, Oxford, UK). The polarized samples were dissolved in a solution of 40-mM TRIS buffer, 50-mM NaCl and 0.1 g/L EDTA-Na<sub>2</sub>, leading to an 80-mM solution of the hyperpolarized substrate with a pH of approximately 7.5.

### In Vivo Experiments

Healthy male Wistar rats (393 ± 48 g body weight, n = 3) were injected with 2.6-3.2 mL of the hyperpolarized solution (target dose = 1 mmol/kg body weight) through a tail vein catheter at a rate of approximately 0.25 mL/s. The time from dissolution to start of injection was approximately 20 s.

The rats were anesthetized initially with 2.5% isoflurane in oxygen (1.5 L/min) for tail vein catheterization. Respiration, rectal temperature, heart rate and oxygen saturation were monitored throughout the experiments with temperature regulated using a warm water blanket placed underneath the animals. Each animal received two injections of the hyperpolarized substrate, approximately 1.5 - 2 h apart. All animal procedures were approved by the SRI Institutional Animal Care and Use Committee.

All experiments were performed on a clinical 3T Signa MR scanner (GE Healthcare, Waukesha, WI), using a custom-built <sup>13</sup>C transmit/receive surface coil (dia = 28 mm) placed over the heart with rat supine. A quadrature volume rat <sup>1</sup>H coil (diameter = 70 mm) was used for anatomical localization and to confirm the position of the <sup>13</sup>C coil with respect to the heart. Single-shot fast spin-echo (FSE) <sup>1</sup>H MR images in the axial, sagittal and coronal planes with nominal in-plane resolution of 0.47 mm and 2-mm slice thickness were acquired as anatomical references for prescribing the <sup>13</sup>C MRS experiments. A non-selective pulse-and-acquire sequence with an excitation flip angle of 6°, spectral width of 5 kHz and 2048 points was used to acquire <sup>13</sup>C spectra from the heart every 3 s over a 4-min period starting at the same time as the [<sup>13</sup>C]-DES injection.

## In Vitro Experiments

*In vitro* experiments were performed in order to facilitate the identification of the metabolites observed from [ $^{13}\text{C}$ ]-DES *in vivo* experiments. These experiments include exposure of [ $^{13}\text{C}$ ]-DES to:

1. Pig Liver Esterase. [ $^{13}\text{C}$ ]-DES (10 mM) was incubated at 37 °C with pig liver esterase (7.5 Units/mL) in RPMI media supplemented with 10% fetal bovine serum and 5% penicillin-streptomycin. Pig liver esterase has been previously shown to selectively cleave a single ester of DES (39). After 5 min, the solution was then analyzed via  $^{13}\text{C}$ -NMR on an 11.7 T instrument to determine the product distribution.
2. Rat blood. Blood draws were performed from healthy male Wistar rats via tail vein catheter. The freshly drawn blood (1 mL) was immediately dosed with [ $^{13}\text{C}$ ]-DES (100 mM) and the solution was incubated at 37 °C. At various times points (1, 5, 20 and 60 min), a 0.25 mL aliquot of the solution was removed, and the sample was quenched with methanol (0.25 mL). Each sample was then analyzed via  $^{13}\text{C}$ -NMR on an 11.7 T instrument to determine the metabolic fate of [ $^{13}\text{C}$ ]-DES.
3. Homogenates of Rat Heart. Rat hearts were obtained from male Wistar rats and samples were maintained at -80 °C. Samples were thawed, homogenized in buffer (210 mM mannitol, 70 mM sucrose, 5 mM MOPS and 1 mM EDTA in  $\text{D}_2\text{O}$ ), and centrifuged at 3000g to obtain desired homogenates. These homogenates were dosed with [ $^{13}\text{C}$ ]-DES (10 mM) and incubated at 37 °C for 5 min. These samples were analyzed at various time points (5, 20, 60 and 300 min) via  $^{13}\text{C}$ -NMR on an 11.7 T instrument to determine the product distribution.

## Results and Discussion

[ $^{13}\text{C}$ ]-DES was successfully formulated for dynamic nuclear polarization through the addition of 20 mM BDPA to 6 M [ $^{13}\text{C}$ ]-DES (neat). The solid-state polarization build-up time constant was  $1517 \pm 91$  s ( $n = 8$ ) with a liquid-state polarization level of 5.5% (Figure 2). The  $T_1$  ( $^{13}\text{C}$ -labeled carbonyls) was found to be 37.9 s in solution at 3 T. No observable toxicity (pulse or respiration) was detected upon i.v. administration of a TRIS-buffered solution containing up to 80 mM [ $^{13}\text{C}$ ]-DES. In addition, no detectable ester hydrolysis of [ $^{13}\text{C}$ ]-DES to yield [1,4- $^{13}\text{C}$ ]-monoethylsuccinate ([ $^{13}\text{C}$ ]-MES) or [1,4- $^{13}\text{C}$ ]-succinate was observed when [ $^{13}\text{C}$ ]-DES was exposed to the dissolution conditions (40-mM TRIS buffer, 50-mM NaCl and 0.1 g/L EDTA- $\text{Na}_2$ , pH = 7.5) for a period of up to 20 min. Furthermore, no hydrolysis was observed during the dissolution process, which requires superheating the frozen sample (see supporting information).

Figure 3 displays a representative (A) spectrum and (B) time-resolved stackplot obtained from a rat heart after i.v. administration of hyperpolarized [ $^{13}\text{C}$ ]-DES. In these experiments, a bolus injection of 80 mM [ $^{13}\text{C}$ ]-DES was performed, and the substrate was observed at 176.4 ppm along with three other distinct signals at 182.5, 177.6, and 172.7 ppm. Lower substrate concentration (40 mM) did not significantly affect metabolites observed or the relative quantities detected. Importantly, our spectra closely resembled the previously

observed product distribution found in the report by Zacharias et. al. on PHIP-mediated hyperpolarization of [1-<sup>13</sup>C, 2,3-*d*<sub>2</sub>]-diethylsuccinate (32). The PHIP study of DES did, however, consistently detect a minor signal at 175.2 ppm, which is not observed in our experiments and was indicated to be fumarate. The previous work assigned the three major signals at 182.5, 177.6, and 172.7 ppm to succinate, malate and aspartate, respectively. Despite the overall similarity of the spectra, we found several inconsistencies with the previous report's assignments: (1) the chemical shifts found in the metabolite reference data did not agree with the assigned spectra (32) and (2) a single resonance was attributed to asymmetric compounds (i.e. malate and aspartate) that should display two resolvable signals due to scrambling of the <sup>13</sup>C label between the C1 and C4 positions (40). Given these issues, we sought to reexamine the fate of [<sup>13</sup>C]-DES *in vivo* and conduct a thorough study to determine the metabolite distribution.

In order to evaluate whether the metabolites observed *in vivo* correspond to products of esterase cleavage (i.e. [<sup>13</sup>C]-MES and/or [1,4-<sup>13</sup>C]-succinate), a reference standard was prepared with a mixture of these products. A sample containing a 2:3:6 ratio of succinate:DES:MES was prepared through treating [1,4-<sup>13</sup>C]-succinate with 1.0 equivalent of trimethylsilyl chloride in ethanol at room temperature (Figure 4). The ratio of metabolites was determined through analysis of the <sup>1</sup>H-NMR of the sample. This standard was then used to reference the MES and succinate carbonyl shifts via <sup>13</sup>C-NMR on an 11.7 T NMR instrument. Both [1,4-<sup>13</sup>C]-succinate (183.7 ppm) and [<sup>13</sup>C]-DES (176.4 ppm) yield a single resonance as they are symmetric molecules. It was discovered that peaks 182.5 and 177.6 ppm correspond to [<sup>13</sup>C]-MES and do not originate from metabolism via the TCA cycle (Figure 3B). Based upon the difference in chemical shifts, [1,4-<sup>13</sup>C]-succinate should be resolvable *in vivo* from the signal corresponding to [4-<sup>13</sup>C]-MES, so we conclude that [1,4-<sup>13</sup>C]-succinate is not forming in detectable quantities during the time frame of the *in vivo* experiment.

DES was developed as agent for hyperpolarized <sup>13</sup>C metabolic imaging because it was hypothesized to cross biological membranes more readily than the parent compound. However, given that esterases are known to be present in the blood (41), we sought to examine whether cleavage of [<sup>13</sup>C]-DES to [<sup>13</sup>C]-MES could occur extracellularly prior to entry into the cytosol or mitochondria. In order to initially confirm that [<sup>13</sup>C]-DES was a substrate for esterases, the substrate was incubated with pig liver esterase. As anticipated, [<sup>13</sup>C]-MES was cleanly formed and two signals (182.5 and 177.6 ppm) were observed. Next, [<sup>13</sup>C]-DES was added to a freshly drawn rat blood sample, and [<sup>13</sup>C]-MES was again rapidly formed in the first 5 min (Figure 5). No signal corresponding to the unknown compound (172.7 ppm) was detected under these conditions.

In order to determine the identity of this unknown metabolite, we sought to generate, isolate and characterize the species via *in vitro* methods. [<sup>13</sup>C]-DES was incubated with homogenates of rat heart tissue. In all trials, conversion to [<sup>13</sup>C]-MES was observed. However, only trace levels of the unknown metabolite at 172.7 ppm were detected, and unfortunately, the product could not be successfully characterized via this process. Furthermore, prostate cancer cells (PC-3) were dosed with [<sup>13</sup>C]-DES (10 mM), but no



metabolic product corresponding to the signal at 172.7 ppm was observed (see supporting information).

In order to assign the unknown signal, a series of succinate-derived compounds were referenced and compared with previously published TCA cycle metabolites (Table 1). As described above, the signal at 172.7 ppm did not coincide with any intermediate of the TCA cycle. The chemical shifts of aspartate and glutamate, which are products typically formed from TCA cycle intermediates, were also not consistent with the unknown metabolite. However, based upon this analysis, the unknown species in the *in vivo* spectra was tentatively assigned to [1,4-<sup>13</sup>C]-succinic anhydride. This assignment was in agreement with the fact that only a single resonance is observed, which would be expected from a symmetrical molecule like [1,4-<sup>13</sup>C]-succinic anhydride. In addition, [1,4-<sup>13</sup>C]-succinic anhydride maintains the carbon skeleton of [<sup>13</sup>C]-DES without performing any C-C bond cleavage steps, which in the TCA cycle would be associated with the loss and subsequent observation of [<sup>13</sup>C]-CO<sub>2</sub> at 125 ppm, which is in fast exchange with [<sup>13</sup>C]-bicarbonate at 161 ppm. Neither resonance was observed in the *in vivo* experiment.

Succinate would be expected to have a relatively slow rate of dehydration under normal physiological conditions (42-43); therefore, it is unlikely that [1,4-<sup>13</sup>C]-succinate converts to [1,4-<sup>13</sup>C]-succinic anhydride. However, monoesters of succinate have been shown to be unstable due to the close proximity of the neighboring carboxyl group (44), which results in the formation of the corresponding anhydrides. Upon formation, [1,4-<sup>13</sup>C]-succinic anhydride should slowly hydrolyze to furnish [1,4-<sup>13</sup>C]-succinate, which may then be metabolized by the TCA cycle but is not observed at detectable levels in our experiments. Further, although studies with hyperpolarized [1,4-<sup>13</sup>C]-succinate anhydride were attempted, immediate hydrolysis of the substrate to yield [1,4-<sup>13</sup>C]-succinate was observed under standard dissolution conditions.

## Conclusions

Although the diester analog, [<sup>13</sup>C]-DES, of [<sup>13</sup>C]-succinate is more adept at crossing cellular membranes, the substrate is not successfully metabolized by the TCA cycle. [<sup>13</sup>C]-DES is initially metabolized to [<sup>13</sup>C]-MES via endogenous esterases, which may occur in the blood rather than the intracellular environment. Further metabolism of the substrate leads to formation of [1,4-<sup>13</sup>C]-succinic anhydride. Contrary to previous reports of PHIP hyperpolarized [<sup>13</sup>C]-labeled DES, TCA cycle-derived metabolites (succinate, malate and aspartate) were not observed. However, the previous work was able to detect [<sup>13</sup>C]-labeled fumarate *in vivo*. Ongoing research efforts are directed towards the development of novel agents that have the ability to monitor *in vivo* TCA cycle metabolism and, in turn, address the current limitations in this field.

## Supplementary Material

Refer to Web version on PubMed Central for supplementary material.

## Acknowledgments

The following grants and funding organizations are acknowledged: NIH grants AA018681, AA005965, AA013521-INIA, EB009070, P41 EB015891, DOD grant PC100427 and GE Healthcare.

## References

1. Golman K, Zandt RI, Lerche M, Pehrson R, Ardenkjaer-Larsen JH. Metabolic imaging by hyperpolarized  $^{13}\text{C}$  magnetic resonance imaging for in vivo tumor diagnosis. *Cancer Res.* 2006; 66:10855–10860. [PubMed: 17108122]
2. Day SE, Kettunen MI, Gallagher FA, Hu DE, Lerche M, Wolber J, Golman K, Ardenkjaer-Larsen JH, Brindle K. Detecting tumor response to treatment using hyperpolarized  $^{13}\text{C}$  magnetic resonance imaging and spectroscopy. *Nat Med.* 2007; 13:1382–1387. [PubMed: 17965722]
3. Ross BD, Bhattacharya P, Wagner S, Tran T, Sailasuta N. Hyperpolarized MR imaging: neurologic applications of hyperpolarized metabolism. *Am J Neuroradiol.* 2010; 31:24–33. [PubMed: 19875468]
4. Park I, Larson PEZ, Zierhut ML, Hu S, Bok R, Ozawa T, Kurhanewicz J, Vigneron DB, VandenBerg SR, James CD, Nelson SJ. Hyperpolarized  $^{13}\text{C}$  magnetic resonance metabolic imaging: application to brain tumors. *Neuro-oncology.* 2010; 12:133–144. [PubMed: 20150380]
5. Day SE, Kettunen MI, Cherukuri MK, Mitchell JB, Lizak MJ, Morris D, Matsumoto S, Koretsky AP, Brindle KM. Detecting response of rat C6 glioma tumors to radiotherapy using hyperpolarized [1- $^{13}\text{C}$ ]pyruvate and  $^{13}\text{C}$  magnetic resonance spectroscopic imaging. *Magn Reson Med.* 2011; 65:557–563. [PubMed: 21264939]
6. Park I, Bok R, Ozawa T, Phillips JJ, James CD, Vigneron DB, Ronen SM, Nelson SJ. Detection of early response to temozolomide treatment in brain tumors using hyperpolarized  $^{13}\text{C}$  MR metabolic imaging. *J Magn Reson Imaging.* 2011; 33:1284–1290. [PubMed: 21590996]
7. Kurhanewicz J, Vigneron DB, Brindle KM, Chekmenev EY, Comment A, Cunningham CH, DeBerarinis RJ, Green GG, Leach MO, Rajan SS, Rizi RR, Ross BR, Warren WS, Malloy CR. Analysis of cancer metabolism by imaging hyperpolarized nuclei: prospects for translation to clinical research. *Neoplasia.* 2011; 13:81–97. [PubMed: 21403835]
8. Brindle KM, Bohndiek SE, Gallagher FA, Kettunen MI. Tumor imaging using hyperpolarized  $^{13}\text{C}$  magnetic resonance spectroscopy. *Magn Reson Med.* 2011; 66:505–519. [PubMed: 21661043]
9. Park JM, Josan S, Jang T, Merchant M, Yen YF, Hurd RE, Recht L, Spielman DM, Mayer D. Metabolite kinetics in C6 rat glioma model using magnetic resonance spectroscopic imaging of hyperpolarized [1- $^{13}\text{C}$ ]pyruvate. *Magn Reson Med.* 2012; 68:1886–1893. [PubMed: 22334279]
10. Karlsson M, Jensen PR, Duus JØ, Meier S, Lerche MH. Development of dissolution DNP-MR substrates for metabolic research. *Appl Magn Reson.* 2012; 43:223–236.
11. Briere JJ, Favier J, Gimenez-Roqueplo AP, Rustin P. Tricarboxylic acid cycle dysfunction as a cause of human diseases and tumor formation. *Am J Physiol Cell Physiol.* 2006; 291:C1114–C1120. [PubMed: 16760265]
12. Cardaci S, Ciriolo MR. TCA Cycle Defects and Cancer: When metabolism tunes redox state. *Int J Cell Biol.* 2012:1–9.
13. Pollard PJ, Wortham NC, Tomlinson IP. The TCA cycle and tumorigenesis: the examples of fumarate hydratase and succinate dehydrogenase. *Ann Med.* 2003; 35:632–639. [PubMed: 14708972]
14. Bayley JP, Devilee P. Warburg tumours and the mechanisms of mitochondrial tumour suppressor genes. Barking up the right tree? *Curr Opin Genet Dev.* 2010; 20:324–329. [PubMed: 20304625]
15. Beal MF. Energetics in the pathogenesis of neurodegenerative diseases. *Trends Neurosci.* 2000; 23:298–304. [PubMed: 10856939]
16. Henry PG, Lebon V, Vaufrey F, Brouillet E, Hantraye P, Bloch G. Decreased TCA cycle rate in the rat brain after acute 3-NP treatment measured by in vivo  $^1\text{H}$ - $^{13}\text{C}$  NMR spectroscopy. *J Neurochem.* 2002; 82:857–866. [PubMed: 12358791]
17. Bubber P, Haroutunian V, Fisch G, Blass JP, Gibson GE. Mitochondrial abnormalities in Alzheimer brain: mechanistic implications. *Ann Neurol.* 2005; 57:695–703. [PubMed: 15852400]



18. Golman K, Zandt RI, Lerche M, Pehrson R, Ardenkjaer-Larsen JH. Metabolic imaging by hyperpolarized  $^{13}\text{C}$  magnetic resonance imaging for in vivo tumor diagnosis. *Cancer Res.* 2006; 66:10855–10860. [PubMed: 17108122]
19. Golman K, Zandt R, Thaning M. Real-time metabolic imaging. *Proc Natl Acad Sci U S A.* 2006; 103:11270–11275. [PubMed: 16837573]
20. Arunachalam A, Whitt D, Fish K, Giaquinto R, Piel J, Watkins R, Hancu I. Accelerated spectroscopic imaging of hyperpolarized C-13 pyruvate using SENSE parallel imaging. *NMR Biomed.* 2009; 22:867–873. [PubMed: 19489035]
21. Wilson DM, Keshari KR, Larson PE, Chen AP, Hu S, Van Criekinge M, Bok R, Nelson SJ, Macdonald JM, Vigneron DB, Kurhanewicz J. Multi-channel metabolic imaging, with SENSE reconstruction, of hyperpolarized [1- $^{13}\text{C}$ ] pyruvate in a live rat at 3.0 tesla on a clinical MR scanner. *J Magn Reson.* 2010; 205:141–147. [PubMed: 20478721]
22. Hurd RE, Yen YF, Mayer D, Chen A, Wilson D, Kohler S, Bok R, Vigneron D, Kurhanewicz J, Tropp J, Spielman D, Pfefferbaum A. Metabolic imaging in the anesthetized rat brain using hyperpolarized [1- $^{13}\text{C}$ ] pyruvate and [1- $^{13}\text{C}$ ] ethyl pyruvate. *Magn Reson Med.* 2010; 63:1137–1143. [PubMed: 20432284]
23. Park JM, Recht LD, Josan S, Merchant M, Jang T, Yen YF, Hurd RE, Spielman DM, Mayer D. Metabolic response of glioma to dichloroacetate measured in vivo by hyperpolarized  $^{13}\text{C}$  magnetic resonance spectroscopic imaging. *Neuro-oncology.* 2013; 15:433–441. [PubMed: 23328814]
24. Schroeder MA, Atherton HJ, Ball DR, Cole MA, Heather LC, Griffin JL, Clarke K, Radda GK, Tyler DJ. Real-time assessment of Krebs cycle metabolism using hyperpolarized  $^{13}\text{C}$  magnetic resonance spectroscopy. *FASEB J.* 2009; 23:2529–2538. [PubMed: 19329759]
25. Park JM, Josan S, Grafendorfer T, Yen YF, Hurd RE, Spielman DM, Mayer D. Measuring mitochondrial metabolism in rat brain in vivo using MR Spectroscopy of hyperpolarized [2- $^{13}\text{C}$ ]pyruvate. *NMR Biomed.* 2013; 1002/nbm.2935
26. Marjanska M, Iltis I, Shestov AA, Deelchand DK, Nelson C, Ugurbil K, Henry PG. In vivo  $^{13}\text{C}$  spectroscopy in the rat brain using hyperpolarized [1- $^{13}\text{C}$ ]pyruvate and [2- $^{13}\text{C}$ ]pyruvate. *J Magn Reson.* 2010; 206:210–218. [PubMed: 20685141]
27. Schroeder MA, Atherton HJ, Dodd MS, Lee P, Cochlin LE, Radda GK, Clarke K, Tyler DJ. The cycling of acetyl-coenzyme A through acetylcarnitine buffers cardiac substrate supply: a hyperpolarized  $^{13}\text{C}$  magnetic resonance study. *Circ Cardiovasc Imaging.* 2012; 5:201–209. [PubMed: 22238215]
28. Gallagher FA, Kettunen MI, Hu DE, Jensen PR, Zandt R, Karlsson M, Gisselsson A, Nelson SK, Witney TH, Bohndiek SE, Hansson G, Peitersen T, Lerche MH, Brindle KM. *Proc Natl Acad Sci.* 2009; 106:19801–19806. [PubMed: 19903889]
29. Clatworthy MR, Kettunen MI, Hu DE, Matthews RJ, Witney TH, Kennedy BWC, Bohndiek SE, Gallagher FA, Jarvis LB, Smith KGC, Brindle KM. Production of hyperpolarized [1,4- $^{13}\text{C}$ ]malate from [1,4- $^{13}\text{C}$ ]fumarate is a marker of cell necrosis and treatment response in tumors. *Proc Natl Acad Sci.* 2012; 109:13374–13379. [PubMed: 22837393]
30. Bhattacharya P, Chekmenev EY, Perman WH, Harris KC, Lin AP, Norton VA, Tan CT, Ross BD, Weitekamp DP. Towards hyperpolarized  $^{13}\text{C}$ -succinate imaging of brain cancer. *J Magn Reson.* 2007; 186:150–155. [PubMed: 17303454]
31. Chekmenev EY, Hövener J, Norton VA, Harris K, Batchelder LS, Bhattacharya P, Ross BR, Weitekamp DP. PASADENA hyperpolarization of succinic acid for MRI and NMR spectroscopy. *J Am Chem Soc.* 2008; 130:4212–4213. [PubMed: 18335934]
32. Zacharias NM, Chan HR, Sallasuta N, Ross BD, Bhattacharya P. Real-time molecular imaging of tricarboxylic acid cycle metabolism in vivo by hyperpolarized 1- $^{13}\text{C}$  diethyl succinate. *J Am Chem Soc.* 2012; 134:934–943. [PubMed: 22146049]
33. Ladriere L, Zhang TM, Malaisse WJ. Effects of succinic acid dimethyl ester infusion on metabolic, hormonal, and enzymatic variables in starved rats. *JPEN J Parenter Enteral Nutr.* 1996; 20:251–256. [PubMed: 8865105]

34. Malaisse WJ, Zhang TM, Verbruggen I, Willem R. Enzyme-to-enzyme channelling of Krebs cycle metabolic intermediates in Caco-2 cells exposed to [2-13C]propionate. *Biochem J.* 1996; 317(Pt3): 861–863. [PubMed: 8760374]
35. Isaacs JS, Jung YJ, Mole DR, Lee S, Torres-Cabala C, Chung YL, Merino M, Trepel J, Zbar B, Toro J, Ratcliffe PJ, Linehan WM, Neckers L. HIF overexpression correlates with biallelic loss of fumarate hydratase in renal cancer: novel role of fumarate in regulation of HIF stability. *Cancer Cell.* 2005; 8:143–153. [PubMed: 16098467]
36. Selak MA, Armour SM, MacKenzie ED, Boulahbel H, Watson DG, Mansfield KD, Pan Y, Simon MC, Thompson CB, Gottlieb E. Succinate links TCA cycle dysfunction to oncogenesis by inhibiting HIF- $\alpha$  prolyl hydroxylase. *Cancer Cell.* 2005; 7:77–85. [PubMed: 15652751]
37. Mitchell M, Cashman KS, Gardner DK, Thompson JG, Lane M. Disruption of mitochondrial malate-aspartate shuttle activity in mouse blastocysts impairs viability and fetal growth. *Biol Reprod.* 2009; 80:295–301. [PubMed: 18971426]
38. Yen YF, Nagasawa K, Nakada T. Promising application of dynamic nuclear polarization for in vivo 13C MR imaging. *Mag Reson Med Sci.* 2011; 10:211–217.
39. Ager DJ, Prakash I. Pig liver esterase catalyzed hydrolyses of diesters. A new route to the syntheses of achiral half-esters. *Synth Commun.* 1995; 25:739–742.
40. Merritt ME, Harrison C, Sherry AD, Malloy CR, Burgess SC. Flux through hepatic pyruvate carboxylase and phosphoenolpyruvate carboxykinase detected by hyperpolarized 13C magnetic resonance. *Proc Natl Acad Sci U S A.* 2011; 108:19084–19089. [PubMed: 22065779]
41. Rudakova EV, Boltneva NP, Makhaeva GF. Comparative analysis of esterase activities of human, mouse, and rat blood. *Bull Exp Biol Med.* 2011; 152:73–75. [PubMed: 22803044]
42. Higuchi T, Miki T. Reversible formation of amides from free carboxylic acid and amine in aqueous solution. A case of neighboring group facilitation. *J Am Chem Soc.* 1961; 83:3899–3901.
43. Chen HT, Chang JG, Musaev DG, Lin MC. Computational study on kinetics and mechanisms of unimolecular decomposition of succinic acid and its anhydride. *J Phys Chem A.* 2008; 112:6621–6629. [PubMed: 18582025]
44. Dörwald, FZ. *Side Reactions in Organic Synthesis.* Wiley-VCH; Weinheim: 2005. and reference therein

## Abbreviations used

<b>TCA cycle</b>	tricarboxylic acid cycle
<b>MRS</b>	magnetic resonance spectroscopy
<b>DNP</b>	dynamic nuclear polarization
<b>PHIP</b>	parahydrogen-induced polarization
<b>DES</b>	diethylsuccinate
<b>MES</b>	monoethylsuccinate

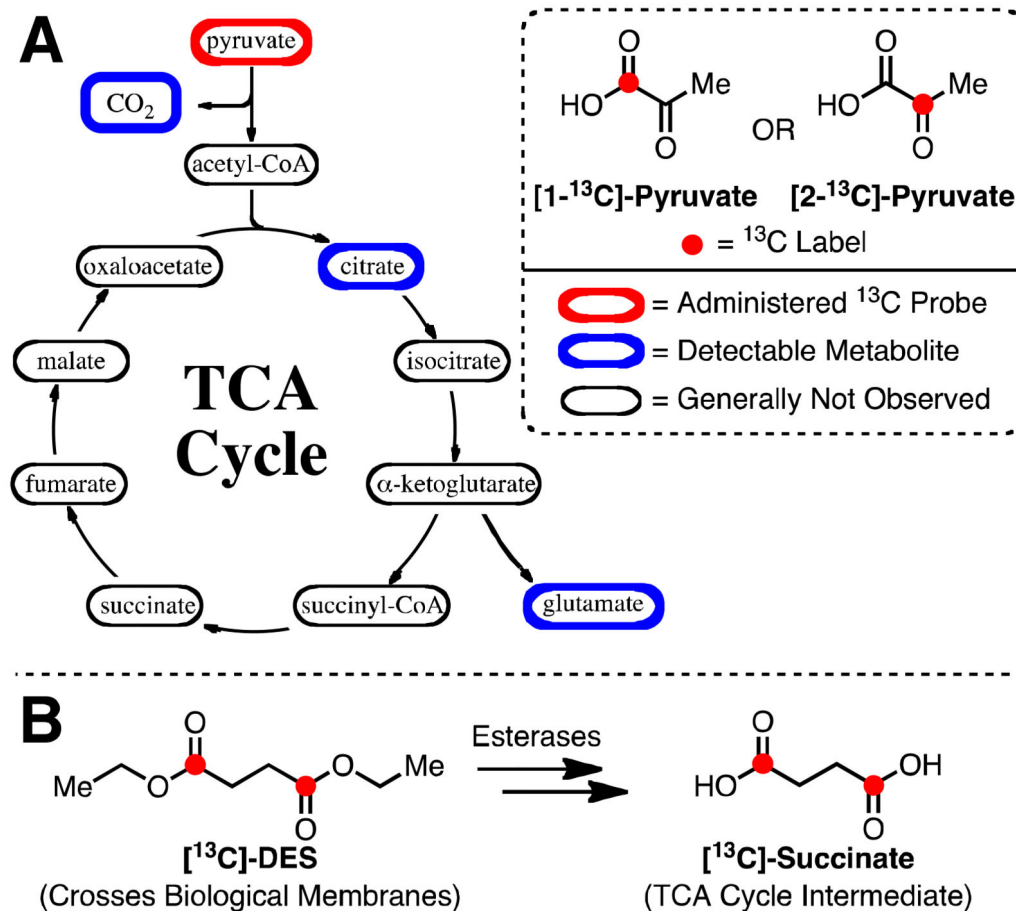


**Figure 1.**

(A) Overview of compounds related to the TCA cycle that are generally detected when employing hyperpolarized [1-<sup>13</sup>C]- or [2-<sup>13</sup>C]-pyruvate. (B) Strategy for probing TCA cycle metabolism. DNP substrate, [<sup>13</sup>C]-DES, enters intracellular environment and is converted into TCA cycle intermediate.

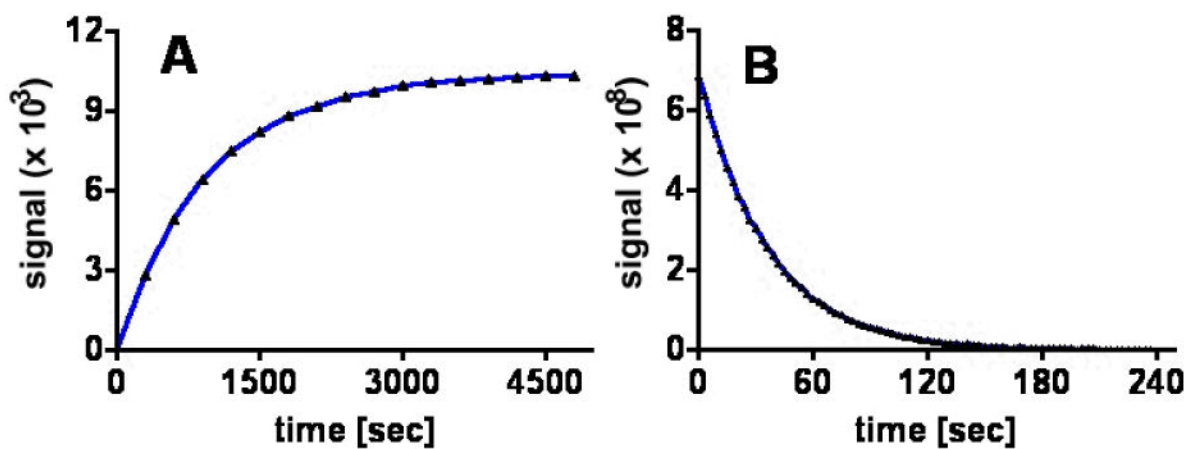
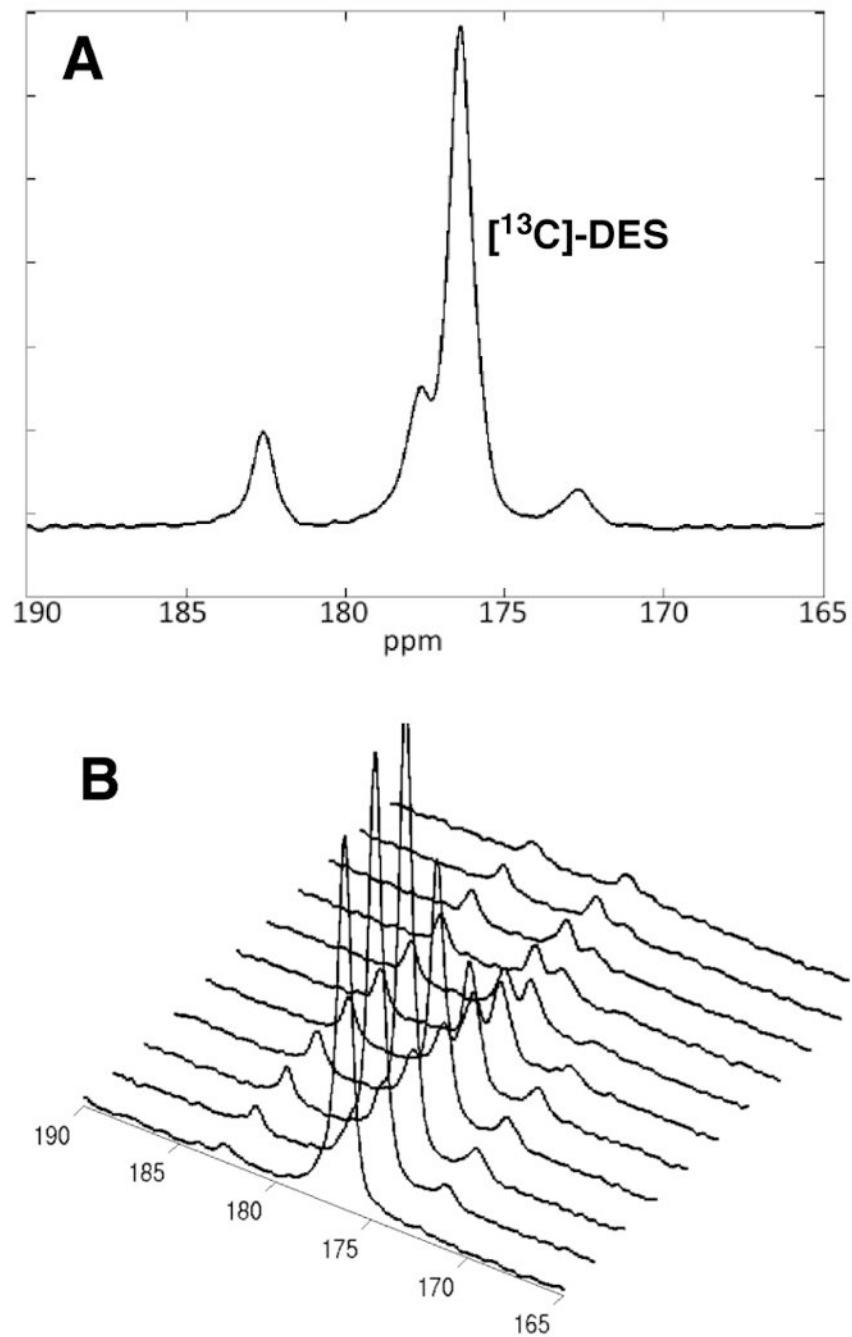


Figure 2.

(A) Polarization buildup curves (3.35 T, 1.4 K) of [<sup>13</sup>C]-DES doped with 20 mM BDPA taken at P(+) = 94.116 GHz. (B) Liquid-state T<sub>1</sub> decay (3 T, 298 K) of [<sup>13</sup>C]-DES samples with 20 mM BDPA (T<sub>1</sub> = 38 s).



**Figure 3.**

(A) Representative time-averaged spectra from 6 - 45 s obtained from heart beginning at the administration of 80 mM  $^{13}\text{C}$ -DES. (B) Representative stackplot of spectra obtained from heart at 3 s intervals beginning at the administration of 80 mM  $^{13}\text{C}$ -DES.

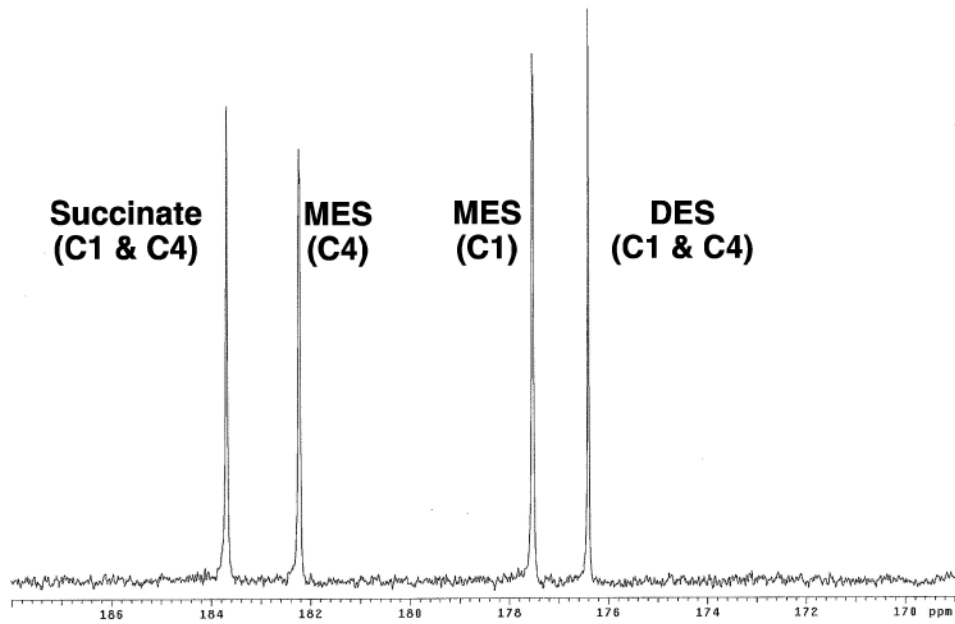
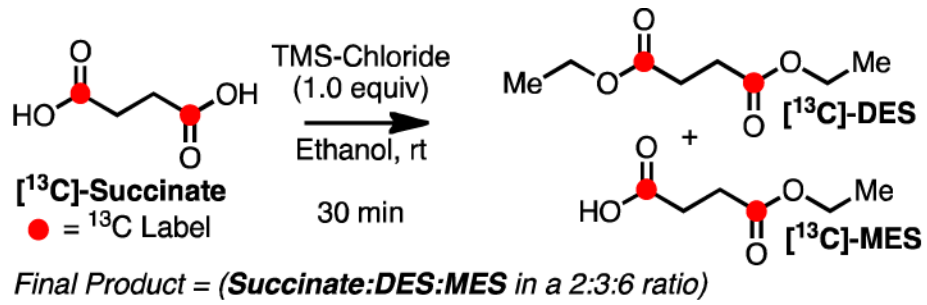


**Figure 4.**

Synthesis of reference sample containing succinate, DES and MES.  $^{13}\text{C}$ -NMR spectrum displays the relative chemical shift of these compounds.



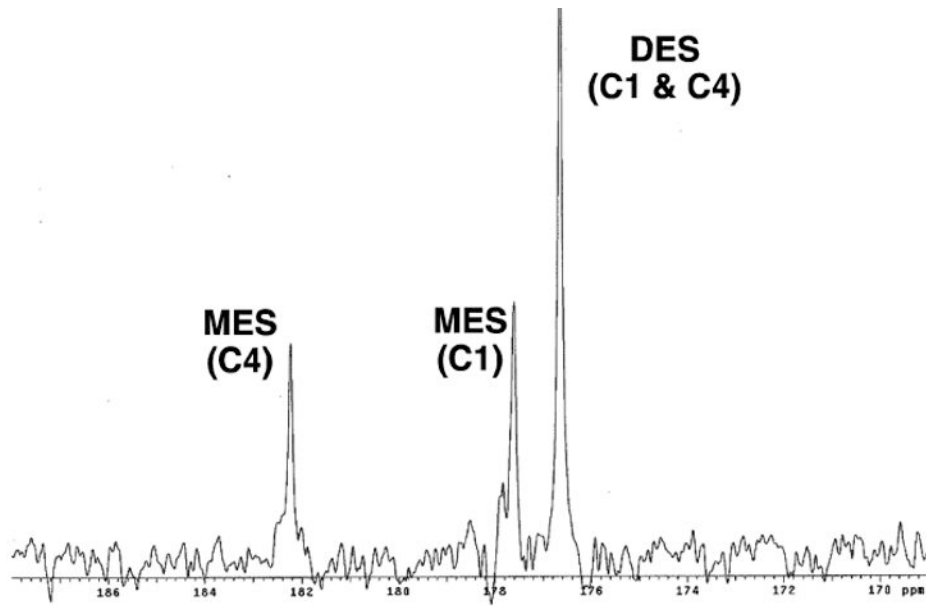


**Figure 5.** Exposure of [<sup>13</sup>C]-DES to rat blood. Representative spectrum (20 min) shown to display the conversion to [<sup>13</sup>C]-MES via endogenous esterases.

**Table 1**

Chemical shifts of TCA cycle intermediates, commonly observed metabolites and succinate-based compounds.

compound	position	pH	<sup>13</sup> C shift
succinate	C1	7.4	183.7 <sup>a</sup>
citrate	C6	7.4	182.5 <sup>b</sup>
monoethylsuccinate	C4	7.4	182.3 <sup>a</sup>
glutamate	C5	7.4	181.8 <sup>C</sup>
malate	C4	7.3	181.6 <sup>b</sup>
isocitrate	C1,C5	7.0	181.4 <sup>b</sup>
isocitrate	C6	7.0	180.7 <sup>b</sup>
malate	C1	7.3	180.4 <sup>b</sup>
citrate	C1,C5	7.4	179.7 <sup>b</sup>
aspartate	C4	7.4	178.5 <sup>C</sup>
monoethylsuccinate	C1	7.4	177.6 <sup>a</sup>
diethylsuccinate	C1	7.4	176.4 <sup>a</sup>
aspartate	C1	7.4	175.3 <sup>C</sup>
fumarate	C1	7.4	175.2 <sup>a</sup>
glutamate	C1	7.4	175.1 <sup>c</sup>
succinic anhydride	C1	7.4	172.8 <sup>a</sup>

<sup>a</sup>Measurements conducted in 100 mM sodium bicarbonate buffer (ionic strength = 0.1) at pH = 7.4 and temperature = 23 °C.

<sup>b</sup>Ref. 32 (temperature = 23 °C).

<sup>c</sup>UT-Southwestern Advanced Imaging Research Center (AICR) metabolite database.